2014 IEEE International Conference on Robotics & Automation (ICRA)
Hong Kong Convention and Exhibition Center
May 31 - June 7, 2014. Hong Kong, China

Development of High Performance Intrinsically Safe 3-DOF Robot

Alex S. Shafer and Mehrdad R. Kermani

Abstract— **In our previous work we have introduced the Distributed Active/Semi-Active actuation concept. This paper presents the design of a novel three Degrees-of-Freedom (DOF) robot manipulator based on the DASA actuation approach. The robot is developed as a proof-of-concept prototype intended to demonstrate the capacity of the DASA approach to achieve a high degree of interaction safety as well as performance. Magneto-Rheological (MR) clutches form the basis of the Semi-active actuation component, while a unidirectional motor provides the active drive for the robot. An antagonistic clutch configuration is implemented at the joints to achieve bi-directional actuation without reversal of the motor. MR clutches have been shown to exhibit excellent torque-to-inertia and torque-to-mass ratios making them likely candidates for the development of human-safe actuators. In this paper, the safety characteristics of the DASA approach are qualitatively discussed. Experimental results highlighting the performance capability of the developed robot are given.**

I. Introduction

Recent years have marked substantial efforts aimed at altering the landscape of automation by promoting access to human safe robotic systems. Direct interaction between humans and robots allows for new collaborative tasks to be defined. Moreover, the advent of safe robots permits a new teaching paradigm based on interactive training. This allows automated production to bypass the expertise and personnel typically required to manage and configure in-house automation systems.

There are several sources of danger when working closely with robotic devices, however collisions between robots and humans pose arguably the largest potential for injury. Such collisions will become unavoidable, if not routine as man and machine continue to integrate into a single working environment.

Our research aims to improve access to human safe robotic systems for small and medium sized enterprizes (SME). Our goal is to balance the competing design requirements of safety and performance while addressing some of the architectural elements that tie cost to performance in this area. We note the performance disparity that exists between *high-end* [1] and *low-cost* [2] automation products developed for interactive application.

A prevailing trend within the research centers around the development of compliant actuators that achieve safety by necessarily compromising performance. Subsequent evolutions improve performance typically at the expense of added complexity. The complexity of actuators has a direct impact on their eventual cost. Ultimately, the balance between safety, performance and complexity appears difficult to obtain with this approach. In our work, we propose an alternative approach based on a class of fully compliant semi-active devices. The devices are based on Magneto-Rheological (MR) fluids and possess excellent performance characteristics. Moreover, such devices have simple mechanical constructions.

The authors are with the Department of Electrical and Computer Engineering at The University of Western Ontario, London, ON, Canada, ashafer2@uwo.ca, mkermani@eng.uwo.ca

Fig. 1. 3-DOF DASA manipulator.

In our previous work [3], we have proposed the Distributed Active Semi Active Actuation Approach (DASA) for human safe robotics. The underlying concept of the DASA approach is the separation of an actuation element into two components, namely an active (e.g. motor) and separate semi-active (e.g. clutch) device. This opens up the possibility of locating the active component in an area that is remote from actuation region; that is to say, a non collocated arrangement. Additionally, the active/semi-active separation allows for multiple semi-active devices to be driven by a single active component.

In this paper, we present the design and experimental results for a 3-DOF implementation of the DASA actuation approach (Fig. 1). The prototype manipulator developed for this purpose is fully compliant although achieves performance levels that are significantly higher than the compliant actuation approaches discussed in the following section.

978-1-4799-3684-7/14/$31.00 ©2014 IEEE

II. Review of Human-Friendly Actuation

A. Joint-Torque Control

For a manipulator to be considered safe for human collaboration, it must be capable of control, as well as limiting interaction forces. In addition, the manipulator inertia must be sufficiently low to prevent injuries resulting from human-robot collision. Manipulators having high inertia can however be safe provided the velocity at which they operate is sufficiently restricted, resulting in strict performance limitations. Stiff manipulators require joint torque sensors to achieve force control. Such manipulators can safely restrict interaction forces below the bandwidth of the torque control loop. Moreover, this class of manipulators can be controlled to exhibit very low mechanical impedance for interactions which have dynamics below the control bandwidth. However, collisions which have dynamics above the bandwidth of the torque control are subject to the open-loop characteristics of the manipulator, which can be dangerous as a consequence of the stiff motor coupling. To be sufficiently lightweight for such applications, motors drives require considerable gear reduction to amplify their output torque. This however, amplifies the output inertia of the motor by the square of the gear ratio. The resulting reflected inertia from the motor develops a substantial contribution towards the manipulator's effective inertia which can often be larger than the inertia developed my the mass of the links.

B. Compliant Actuators

Compliant actuators dynamically decouple the reflected actuator inertia from the link by integrating an elastic [4] and/or damper [5] into the motor's transmission. This inherently improves the collision safety, however degrades the position accuracy and control bandwidth of the actuator [6]. In response to this, variable stiffness [7] and variable impedance actuators [8] have been developed, which can dynamically vary their coupling parameters (i.e. stiffness/damping). Such actuators can increase coupling stiffness at low velocities when a higher effective inertia is tolerated without degrading safety. In this way, control performance is improved at low velocities. This approach require additional actuators to vary coupling parameters and increases the mechanical complexity of implementation. The Distributed Macro-Mini Actuation approach (DM^2) [9], [10], [11] was proposed as an alternative approach to address the performance shortfall of compliant actuators. Actuation of the joint is achieved by the coupling of a low frequency high torque series elastic actuator (SEA) with a high frequency low torque servo. The high frequency servo is directly coupled to the joint and used to actuate the manipulator in a complimentary frequency space to that of the SEA. In this way, the effective controllable bandwidth of the manipulator is improved. The low torque-high frequency servo is selected such that its output inertia is minimized. Thus, safety is maintained while performance is improved. This approach again requires additional motors, as well as a more elaborate form of transmission to combine the two actuators. In general, a trend can be identified in which improving the performance of this class of compliant actuators is achieved at the cost of increasing complexity. In addition, elastic elements have the capacity to store energy during collisions. This adds another level of complexity as this energy must be safely dissipated.

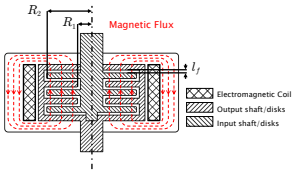

Fig. 2. Cross-section of a multi-disk style MR clutch and its corresponding magnetic circuit.

III. Distributed Active Semi-Active Actuation Approach

The DASA approach is implemented using antagonistic MR clutches to actuate the joints. MR fluids are a suspension of micrometer-sized particles in a carrier fluid. When subjected to a magnetic field, the particles aggregate into columns aligned in the direction of the field. Subsequently, the columns act to resist shearing of the fluid perpendicular to the field. The apparent yield stress of the fluid is dependant on, and increases with the intensity of the applied magnetic field. Fig. 2 shows the cross-section of a multi-disk style MR fluid clutch. MR fluid fills the volume between input and output disks. Rotation of the input shaft causes shearing in the fluid with respect to the output shaft. By energizing the electromagnetic coil, a field is induced in the MR fluid altering its apparent yield strength. The transmission torque of an MR clutch is derived from the Bingham visco-plastic model [12] and is given by

$$T_{MRC} = f(H)\,\mathrm{sgn}(\dot{\theta} - \dot{q}) + b_v(\dot{\theta} - \dot{q}), \tag{1}$$

where H is the intensity of the applied magnetic field, $f(\cdot)$ is the field dependant transmission torque, b_v is the damping coefficient resulting from the viscosity of the MR fluid, and $\dot{\theta}$ and $\dot{q}$ are the absolute angular velocities of the input and output ports of the clutch, respectively. An antagonistic arrangement is achieved by coupling together the output from two clutches. Because the clutches can only transmit torque in the direction that they are driven relative to the output, we designate a *positive* and *negative* clutch which should thus be driven accordingly -that is to say in opposite directions with respect to the output. Assuming the clutches share identical parameters, the combined output torque is given by

$$\begin{aligned} T_{A-MRC} \quad = \quad & f(H^+)\,\mathrm{sgn}(\dot{\theta}^+ - \dot{q}) \\ & + f(H^-)\,\mathrm{sgn}(\dot{\theta}^- - \dot{q}) - 2b_v\dot{q}, \end{aligned} \tag{2}$$

where the superscripts $^+$ and $^-$ indicate parameters belonging to the positive and negative clutch respectfully. Here, it is assumed that $\dot{\theta}^+ \geq 0$ and $\dot{\theta}^+ = -\dot{\theta}^-$.

In contrast to the compliant actuators discussed in the previous section, actuation by antagonistic MR clutch exhibits no elastic or viscous coupling between the input and output.

TABLE I

SPECIFICATIONS OF THE 3-DOF DASA ROBOT

	Length	Mass
Link 1	-	31.79 kg
Link 2	0.3 m	7.07 kg
Link 3	0.435 m	1.88 kg

TABLE II

SPECIFICATIONS OF MR CLUTCHES

	Joint 2	Joint 3 †
Output Torque [Nm]	136	36
Mass [kg]	4.9	1.8

† Joints one and three clutches have equivalent specifications.

Thus, actuation of a joint by an antagonistic MR clutch fully decouples the link from the reflected inertia of the driving motor. As MR clutches can be designed to achieve excellent bandwidth, the decoupling does not come at the expense of performance.

As discussed earlier, force/torque control is an important element of physical human robot interaction. However, the integration of joint-torque sensors to achieve this goal adds considerable mechanical complexity as well as cost. To their benefit, MR clutches offer an alternative method by which to measure the actuator torque. As the transmission torque developed by an MR clutch is proportional to the magnetic field at the fluid, measurement of this field thus allows for close estimation of the resulting torque. The use of Hall sensors for the purpose of torque-sensorless control an MR clutch is covered in [13], [14], [15].

IV. DESIGN OF 3-DOF DASA ROBOT

In this section we present the design of the developed 3-DOF DASA robot (Fig. 3). Key specifications of the manipulator and clutches are given in Table I and Table II respectively. Although the combined mass of the robot is substantial, much of this mass is located at the base of the robot which is subject only to rotation and does not move about the workspace. Additionally, the mass distribution in the first link is concentrated at the axis of rotation to minimize inertia. The flying mass of the robot, that is the mass of the robot that undergos translational movement is only 8.95 kg. The distinction is important as this mass comprises the significant portion of the manipulator's effective inertia. The mechanical drive for the robot is provided by a single motor coupled through a gearbox. The drive assembly, which includes the motor and gearbox is located at the base of the robot in order to minimize the manipulator's inertia. This permits the use of heavier off-the-shelf components that are less costly as they are not optimized for low-weight applications. The brushless DC motor that drives the robot is produced by Hacker, model A60-18. The motor has a mass of 910 g and produces a peak power of 2.6 kW, sufficient to power all three joints of the robot.

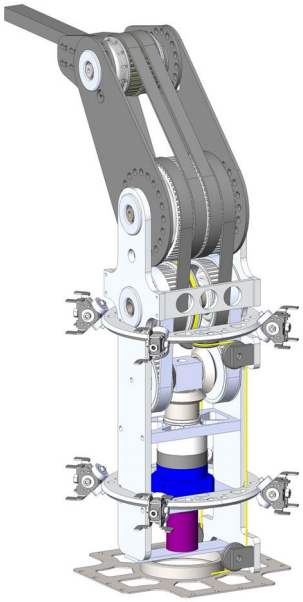

Fig. 3. Rendering of the 3-DOF DASA manipulator.

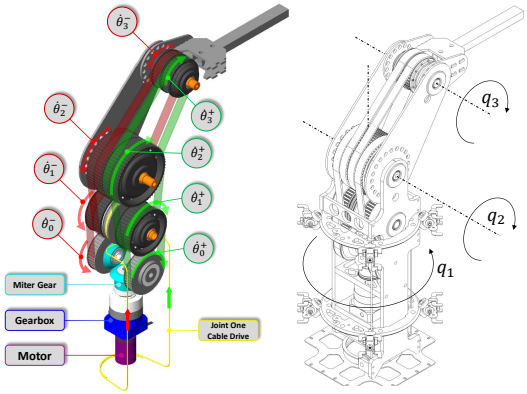

Fig. 4. Transmission model and joint definition of the 3-DOF DASA manipulator. Clutch input velocity is given by $\dot{\theta}_i^{\pm}$. Arrow heads indicate positive direction.

A. Transmission

The use of a single motor to simultaneously drive all three joints of the manipulator is achieved using a serially coupled belt transmission, shown in Fig. 4. The output of the gearbox drives a set of miter gears that produce rotation in both clockwise (CW) and counterclockwise (CCW) directions. The miter gears drive two sets of timing belts shown in green and red in Fig. 4. The green belts provide CW rotation to the joints, while the red belts provide CCW rotation. The output of the joint two and three clutches is directly coupled to the subsequent link by an adjoining shaft (see Fig. 6). The output from the joint one clutches drive a winch that winds high strength steel cable around a stationary cylinder at the base of the robot. The cable is shown in yellow in Fig. 4. This mechanism allows the first joint to rotate about the axis normal to the ground.

B. Control

Control of the DASA manipulator concerns joint torques, as well as motor velocity. The torque produced by an antagonistic MR clutch as given in (2) assumes that the input velocity of the two clutches is equal in magnitude and opposite in direction, $\dot{\theta}^+ = -\dot{\theta}^-$. Due to the implementation of the serial transmission, the input ports of the joint three clutches experience a velocity differential caused by rotation in the second joint. In order to derive the actuation model for the DASA manipulator, we model the transmission in terms of $\dot{\theta}_i^+$ and $\dot{\theta}_i^-$ which represent the angular velocity at the input of the positive (CW-driven) and negative (CCW-driven) clutches respectively, of joint i (refer to Fig. 4). We define $\dot{\theta}_0$ to be the angular velocity of the motor as measured after the gearbox. The relationship between the motor velocity and the clutch input velocity at the joints is given by

$$\begin{bmatrix} \dot{\theta}_1^{\pm} \\ \dot{\theta}_2^{\pm} \\ \dot{\theta}_3^{\pm} \end{bmatrix} = \pm \underbrace{\begin{bmatrix} n_{\frac{0}{1}} \\ n_{\frac{0}{2}} \\ n_{\frac{0}{3}} \end{bmatrix}}_{N} \dot{\theta}_0 + \underbrace{\begin{bmatrix} 0 \\ 0 \\ -n_{\frac{2}{3}}\dot{q}_2 \end{bmatrix}}_{\lambda_N(\dot{q})} \tag{3}$$

(4)

where $\dot{q}_i$ are joint velocities and $n_{\frac{i}{j}} = \frac{R_i}{R_j}$ are gear ratios defined between joints i and j, where R_i and R_j are the radii of the pulleys at joints i and j respectively. Thus, the i^{th} element of the constant vector N contains the drive ratio defined between the motor's output and the clutch input of the i^{th} joint. R_0 is the radius of the drive pulleys which couple the output of the gearbox to the belt transmission. The effect of the kinematic coupling on the serial transmission is accounted for by $\lambda_N(\dot{q})$. Note that joints $i = 1, 2$ do not experience kinematic coupling and have symmetric input transmissions where $\dot{\theta}_i^+ = -\dot{\theta}_i^-$ at all times. The joint torques produced by the antagonistic MR actuation of the DASA manipulator can thus be given by

$$\begin{aligned} \tau_i = \; & \operatorname{sgn}(\dot{\theta}_i^+ - \dot{q}_i)\, \tau_i^+ + \operatorname{sgn}(\dot{\theta}_i^- - \dot{q}_i)\, \tau_i^- \\ & + b_i(\lambda_{N_i}(\dot{q}) - 2\dot{q}_i), \end{aligned} \tag{5}$$

where τ_i^+ and τ_i^- are non-negative field dependant transmission torques developed by the the positive and negative clutch respectively, b_i is the (matched) viscous damping coefficient and the subscript i denotes the joint. In order for the torque τ_i^+ to be applied in the positive direction, the motor velocity must satisfy $(\dot{\theta}_i^+ - \dot{q}_i) > 0$ for all joints. Similarly, for the torque τ_i^- to be applied in the negative direction, $(\dot{\theta}_i^- - \dot{q}_i) < 0$ must be satisfied. Using the relationship given in (3), it is straightforward to find the minimal motor velocity θ_0 that satisfies the stated conditions.

C. Design of MR Clutch

Design of the robot is based on an integrated approach such that the clutches are assembled directly onto the output shaft. The shaft material is used by the clutch to form the core of the magnetic circuit. Fig. 6 shows the antagonistic clutches integrated onto the shaft of joints one and two. The clutch

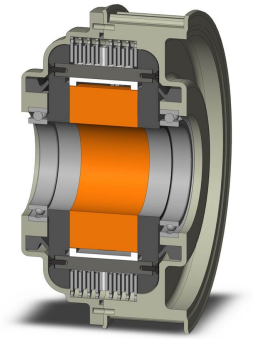

Fig. 5. Cross-section of joint three MR Clutch.

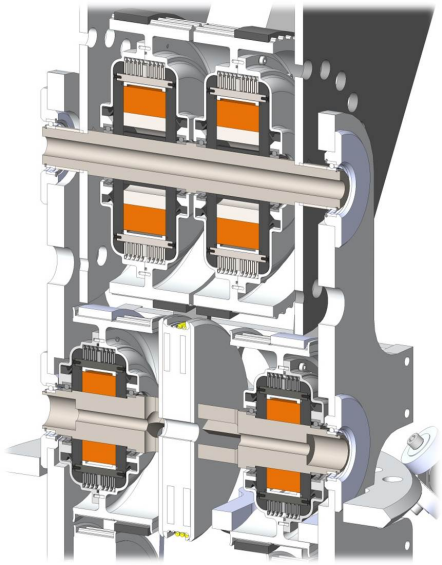

Fig. 6. 3DOF DASA manipulator showing MR clutches integrated onto the joint shaft.

assembly is integrated directly into the timing pulley (see Fig. 5). The pulley forms the input ports to the clutch, and the output shaft forms the output. Clutch geometries were determined using FEM based magnetic circuit optimization in which the mass of the clutch is minimized for a required design torque.

The clutch pack is constructed from an arrangement of steel disks. Spacers fabricated using a low cost 3D printing process are placed between disks to ensure consistent gap widths. Titanium pins are used to transfer the torque from the output disks to the side plates which are coupled to the output shaft. The pins must be made from a non-ferrous material, however care must be taken to match the mechanical properties to that of the disks. Aluminum is avoided as it has a substantially lower surface hardness than that of steel from which the disks are made. Use of such material may lead to the formation of grooves on the pins' surface that would manifest as backlash in fine control reversals.

Each clutch is designed to integrate two analog and

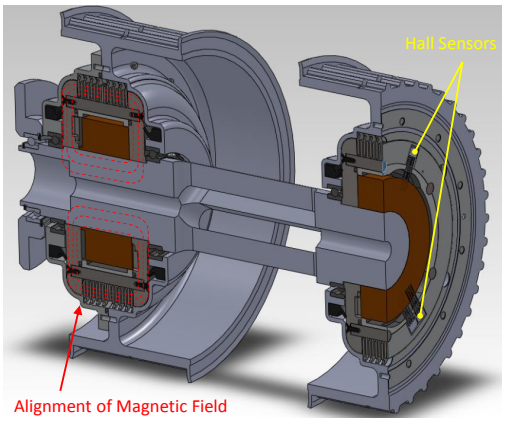

Fig. 7. Cross section of joint one MR clutches showing location of Hall sensors and geometry of magnetic circuit.

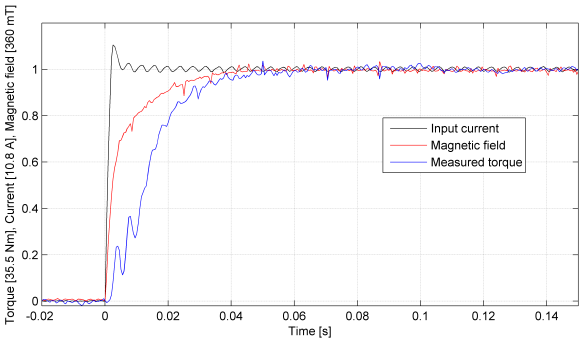

Fig. 8. Normalized step response of joint three clutch. Step size of 35.5 Nm corresponds to 98.6% of the clutch design torque.

two digital Hall sensor assemblies. Analog assemblies are comprised of two unipolar ratiometric Hall sensors (model TLE4990, Infinion) oriented to face in opposite directions. The analog sensors are soldered to a small circuit board with conditioning electronics. The analog Hall sensors provide a combined range of ± 400 mT. A single bipolar digital Hall sensor (model TLE4998, Infinion) and circuit board comprise the digital assemblies. The digital sensors provide a range of ± 200 mT. Sensor assemblies are installed at the axial center of the disk-pack at 90^0 intervals from one another. The four sensors are radially distributed over the active region of the disk pack. The radial distribution allows for measurement of variations in the radial distribution of the magnetic field. Fig. 7 shows a cross section of the MR clutch and the relative locations of the Hall sensor. The details of the Hall sensor integration are reported to provide an understanding of our implementation in the context of a mechanical discussion. Details related to the control as well as results of this method will be reported in upcoming publications.

V. Preliminary Experimental Results

In our previous work [16], we have reported on the high bandwidth that can be achieved in the torque control of MR clutches. Fig. 8 shows the torque step response of the third

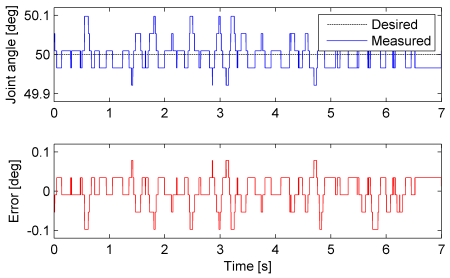

Fig. 9. Joint 2 position regulation control results.

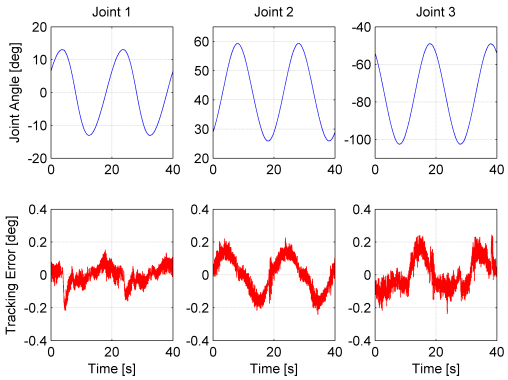

Fig. 10. Position tracking response for sinusoidal input.

joint MR clutch. The step command represents 98.6% of the clutch's design torque (at the third joint). From the plot, we can determine the time constant of the magnetic field to be less than 3.5 ms, and the time constant of the torque response to be about 14 ms.

The high control bandwidth allows MR actuators to perform very well in terms of position control. Fig. 9 shows the results of the 3-DOF DASA Arm commanded to regulate a fixed position. We note that the regulation error is mostly contained between one to two increments of the encoder.

Fig. 10 shows the tracking response of all three joints given sinusoidal inputs. Note that responses shown are produced simultaneously. For this experiment, the motor velocity was held at a constant velocity sufficiently high to satisfy the control requirements discussed in the previous section. We note good tracking performance with error generally confined to $\pm 0.2^0$.

To demonstrate the tracking response at higher frequencies, Fig. 11 shows the response of the third joint commanded to track a 10 Hz sinusoid having a Pk-Pk amplitude of 10^0. Fig. 12 gives the response for a 17 Hz sinusoid with a Pk-Pk amplitude of 5^0. Although the tracking error begins to degrade at higher frequencies, the results indicate the capacity of the antagonistic MR actuator to operate at higher frequencies.

VI. Discussion

As we have shown, the DASA concept allows for a single motor to drive multiple joints of a robot manipulator. As an

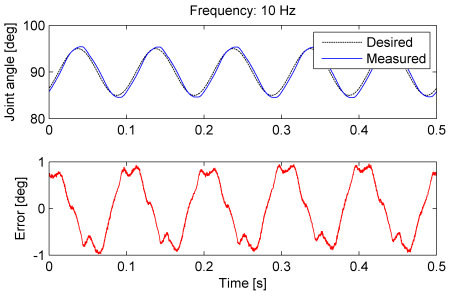

Fig. 11. Joint 3 position tracking control results for sinusoidal input.

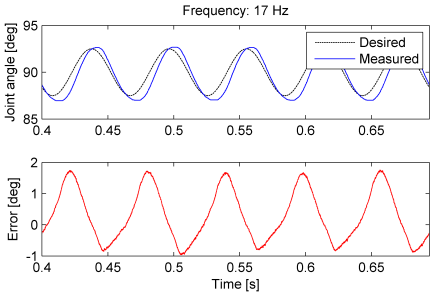

Fig. 12. Joint 3 position tracking control results for sinusoidal input.

example of the design versatility of the DASA architecture, we note that the motor installed in the 3-DOF robot is intended for remote control hobby aircraft. Such low cost motors can successfully drive multiple joints of a robot and do not require any specific performance characteristic outside of power output. The DASA approach is able to bridge the high performance achieved by stiff joint-torque controlled manipulators with the inherent safety of compliant actuators. A limitation of the current design springs from the mass of the clutches. Future work should focus on reducing the clutch mass in order to improve safety characteristics.

REFERENCES

[1] R. Bischoff, J. Kurth, G. Schreiber, R. Koeppe, A. Albu-Schäffer, A. Beyer, O. Eiberger, S. Haddadin, A. Stemmer, G. Grunwald *et al.*, "The kuka-dlr lightweight robot arm-a new reference platform for robotics research and manufacturing," in *Robotics (ISR), 2010 41st International Symposium on and 2010 6th German Conference on Robotics (ROBOTIK)*. VDE, 2010, pp. 1–8.

[2] R. Robotics, "Baxter product page." [Online]. Available: http://www.rethinkrobotics.com/index.php/products/baxter/

[3] A. S. Shafer and M. R. Kermani, "On the feasibility and suitability of mr fluid clutches in human-friendly manipulators," *Mechatronics, IEEE/ASME Transactions on*, vol. 16, no. 6, pp. 1073–1082, 2011.

[4] G. Pratt and M. Williamson, "Series elastic actuators," in *Proc. IEEE/RSJ Int. Conf. Intell. Robot. Syst.*, vol. 1, 1995, pp. 399–406.

[5] C.-M. Chew, G.-S. Hong, and W. Zhou, "Series damper actuator: a novel force/torque control actuator," in *Proc. 4th IEEE/RAS Int. Conf. Humanoid Robot.*, vol. 2, 2004, pp. 533–546.

[6] K. Kong, J. Bae, and M. Tomizuka, "Control of rotary series elastic actuator for ideal force-mode actuation in human-robot interaction applications," *IEEE/ASME Trans. Mechatronics*, vol. 14, no. 1, pp. 105–118, 2009.

[7] G. Tonietti, R. Schiavi, and A. Bicchi, "Design and control of a variable stiffness actuator for safe and fast physical human/robot interaction," in *Proc. IEEE Int. Conf. Robot. Autom.*, 2005, pp. 526–531.

[8] A. Bicchi and G. Tonietti, "Fast and soft arm tactics: Dealing with the safety-performance trade-off in robot arms design and control," *Robotics Automation Magazine, IEEE*, vol. 11, no. 2, pp. 22–33, 2004.

[9] M. Zinn, O. Khatib, B. Roth, and J. K. Salisbury, "A new actuation approach for human friendly robot design," in *International Symposium on Experimental Robotics, S. Angelo dIschia, I*, 2002, pp. 379–398.

[10] M. Zinn, O. Khatib, and B. Roth, "A new actuation approach for human friendly robot design," in *Proc. IEEE Int. Conf. Robot. Autom.*, vol. 1, 2004, pp. 249–254.

[11] M. Zinn, "A new actuation approach for human friendly robot manipulation," Ph.D. dissertation, Stanford University, Stanford, CA, 2005.

[12] R. W. Phillips, "Engineering applications of fluids with a variable yield stress," Ph.D. dissertation, University of California, Berkeley, 1969.

[13] A. Shafer and M. R. Kermani, "Magneto-rheological clutch with sensors measuring electromagnetic field strength," Oct. 8 2010, wO Patent App. PCT/CA2010/001,577.

[14] A. SHAFER, M. KERMANI *et al.*, "Magneto-rheological clutch with sensors measuring electromagnetic field strength," Apr. 15 2011, wO Patent 2,011,041,890.

[15] A. Shafer and M. R. Kermani, "Magneto-rheological clutch with sensors measuring electromagnetic field strength," Feb. 28 2013, uS Patent 20,130,047,772.

[16] A. S. Shafer and M. R. Kermani, "Design and validation of a magneto-rheological clutch for practical control applications in human-friendly manipulation," in *Robotics and Automation (ICRA), 2011 IEEE International Conference on*. IEEE, 2011, pp. 4266–4271.